# Magnetoresistance of Nanosized, Granular $Sr_2FeMoO_{6-\delta}$–$SrMoO_4$ Core–Shell Structures

*Gunnar Suchaneck\* and Evgenii Artiukh*

Herein, for the first time, a model is developed for the description of magnetoresistance in nanosized, granular $Sr_2FeMoO_{6-\delta}$–$SrMoO_4$ core–shell structures, which is based on the fluctuation-induced tunneling model. Parameters of the fluctuation-induced tunneling model of granular materials are calculated. The magnetic field is considered to affect the tunneling barrier height. The linear and quadratic coefficients of this effect are estimated.

## 1. Introduction

The transport properties of $Sr_2FeMoO_6$ (SFMO) depend significantly on sample microstructure. Usually, SFMO ceramics are synthesized and annealed at temperatures in the order of 1200 °C.[1–5] Thereby, cationic ordering increases up to 1200 °C with increasing sintering temperature improving also magnetic properties.[3] The main contribution to the low-field magnetoresistance (MR) absence in single crystals[2] arises from tunneling magnetoresistance (TMR) between ferromagnetic metallic regions separated by insulating barriers.[1,2,4,5] On the contrary, antiphase boundaries (APBs) serving as barriers for intragrain tunneling are still present after annealing at 1200 °C. APBs contribute significantly to the TMR till a perceptible amount of APBs exist. Just annealing at 1500 °C practically removes all the APBs.[6]

Low-temperature annealing of SFMO leads to the formation of $SrMoO_4$ (SMO) grain boundaries which modifies the TMR of this material.[7,8] After annealing at 1100 °C, the dissolution of SMO takes place improving Fe/Mo ordering and enhancing the intergranular TMR.[6] In annealed below 900 °C samples,

magnetically distorted grain boundaries possessing spin-glass properties were obtained.[6] In this case, a spin-valve-like magnetoresistivity appears.

Another possibility of realizing large TMRs is granular materials in the superparamagnetic state.[9] Here, spin scattering at grain boundaries depends on the direction of the conduction electron's spin with respect to the direction of the magnetic moments. In the superparamagnetic state, the tunnel current is different whether $B$ is zero or applied because, at $B = 0$, tunneling electrons with both spins meet randomly oriented magnetic moments, while at $B \gg 0$ they meet highly oriented magnetic moments, so that the tunneling probability is small at $B = 0$ and large at $B \gg 0$.

In this work, we consider SFMO ceramics comprising nanocontacts between metallic grains. Such samples consist of cold-pressed SFMO,[10] doped cold-pressed SFMO,[11] sintered and granular SFMO,[12] grinded and sintered $Sr_2CrMoO_6$,[13] grinded and sintered as well as cold-pressed $Sr_2FeReO_6$, cold-pressed $Sr_2CrReO_6$ and cold-pressed $Sr_2CrWO_6$,[14] $Ba_2FeMoO_6$ thin films comprising crystalline grains with disordered grain boundary regions,[15] and nanosized, granular SFMO–SMO core–shell structures.[16]

Each of the listed tunneling processes requires an adapted model. A phenomenological model to explain the magnetic field dependence of resistance in granular colossal MR materials was developed.[17] The resistance was considered to consist of three parts: a magnetic field-independent part coming from nonmagnetic defects and phonon scattering, a field-dependent part coming from spin-polarized tunneling, and a field-dependent part coming from the reduction of spin fluctuation. The field dependence of the part coming from spin-polarized tunneling was modeled in terms of a 1D pinning strength $B_{pin}$ taken as the free energy gradient at the domain wall divided by the saturation magnetization, such that for $B \geq B_{pin}$ a domain boundary slips from the grain boundary giving rise to a resistance drop. However, neither final field derivative $d(MR)/dB$ nor any term of it followed the experimental results of SFMO thin films deposited onto various single-crystal substrates.[18] Another phenomenological model for manganites and ferromagnetic alloys[19] is founded on the decomposition of MR into two distinct components: the low-field and high-field MR at a given temperature both represented as $MR \propto B^q/(B_c{}^q + B^q)$. Here, $B_c$ is a critical field at which the value of the MR has fallen by half and $q$ is an exponent which is different for the low- and high-field MRs. For experimental data of $(Ba_{0.8}Sr_{0.2})_2FeMoO_6$ measured up to 50 T,[20] the MR above a critical field of 0.65 T is well fitted to the phenomenological model assuming $MR_{max} = -41.4\%$. On the contrary,

Dr. G. Suchaneck, E. Artiukh
Solid State Electronics Laboratory
TU Dresden
01062 Dresden, Germany
E-mail: gunnar.suchaneck@tu-dresden.de

E. Artiukh
Cryogenic Research Division
SSPA "Scientific-Practical Materials Research Centre of NAS of Belarus"
220072 Minsk, Belarus

The ORCID identification number(s) for the author(s) of this article can be found under https://doi.org/10.1002/pssb.202000629.

the precise physical meaning of the exponent $q \approx 0.8$ remains unclear. Also, the temperature dependence of the MR is not a model component.

The MR of high-temperature synthesized SFMO ceramics is well described by a model introducing a field dependence of the reduced magnetization at the grain boundaries in a functional form $m_{GB} = [1-(B_0/B)^{1/2}]$ obtained earlier for spin glasses with weak anisotropy.[20] Later, the fit to experimental data in the low-field region was improved by adding a tanh-function correction.[21] However, both models fail to describe the MR of nano-sized, granular SFMO–SMO core–shell structures.

In this work, we develop for the first time a model of the MR for the special group of ceramics subjected to fluctuation-induced tunneling (FIT), e.g., for nanosized, granular SFMO–SMO core–shell structures.

## 2. Theory

Usually, SFMO ceramics show an upturn of resistivity at low temperatures (the upturn is missing in single-crystalline samples[2]) to an *increasing* with temperature $\rho(T)$.[1] The resistivity above the upturn temperature of these samples is described by a model of spin-dependent tunneling in granular magnetic films,[20,21] resulting in

$$\rho = \frac{\rho_0 \cdot \exp(f\chi w)}{1 + m^2(B,T) \cdot P(T)^2} \tag{1}$$

where $f$ is a barrier shape factor, $\chi$ is the reciprocal localization length of the wave function, $w$ is the barrier width, $m$ is the relative magnetization, i.e., the magnetization $M$ scaled to the saturation magnetization $M_s$, $T$ is the temperature, $B$ is the magnetic flux density, and $P$ is the spin polarization in the magnetic grains. Here, both $m(B,T)$ and $P(T)$ decrease with temperature, while the tunneling process is temperature independent. In the limit of zero coercive field and an independent on $B$ barrier height, this yields the well-known MR

$$MR = -\frac{m^2(B,T)P^2(T)}{1 + m^2(B,T)P^2(T)} \tag{2}$$

Let's now consider cold-pressed or low-temperature annealed SFMO comprising nanocontacts between metallic grains which form a capacitance $C$ at the intergrain junctions. In such a system, thermal fluctuations occur when the electrostatic energy per electron, $e^2/2C$, is much smaller than the thermal one, $kT/2$, with $e$ the electron charge and $k$ the Boltzmann constant. The random mean square noise voltage generated on an ideal capacitor in an RC circuit is then given by the square root of $kT$ divided by the capacitance $C$.[22] For a dielectric constant of 40, a barrier thickness $d$ of 2 nm, and a contact area $A$ of 400 $nm^2$, the junction capacitance $C$ will be in the order of 0.1 fF. This yields a ratio $e^2/(CkT)$ in the order of 0.1 in the temperature region 50–300 K.

Conducting grains separated by energy barriers subjected to large thermal fluctuations are modeled by the FIT model.[23] The FIT model links the independent on temperature tunneling conductivity[24] with a temperature-dependent conductivity obtained for the tunneling of spin-polarized electrons in granular metal films.[25] It is specified by two parameters:

1) the temperature $T_1$ characterizing the electrostatic energy of a parabolic potential barrier

$$kT_1 = \frac{A \cdot w \cdot \varepsilon_o E_0^2}{2} \tag{3}$$

where the characteristic field $E_0$ with $\varepsilon_0$ the vacuum permittivity is determined by the barrier height $V_0$

$$E_0 = \frac{4V_0}{e \cdot w} \tag{4}$$

and 2) the temperature $T_0$ representing $T_1$ divided by the tunneling constant

$$T_0 = T_1 \cdot \left(\frac{\pi\chi w}{2}\right)^{-1} \tag{5}$$

with the reciprocal localization length of the wave function

$$\chi = \sqrt{\frac{2m^* V_0}{\hbar^2}} \tag{6}$$

where $m^*$ is the effective electron mass and $\hbar$ is the Planck constant expressed in J s radian$^{-1}$. Note that Equation (3) can be written in a more generalized form

$$T_0 = \frac{T_1}{f\chi w} \tag{7}$$

where $f$ is the shape factor introduced earlier.

The resulting by this model resistivity yields

$$\rho(T) = \rho_0 \exp\left(\frac{T_1}{T_0 + T}\right) \tag{8}$$

i.e., the samples possess a *decreasing* with temperature resistivity.[10–16] At $T \ll T_0$ (large electrostatic energy), the conductivity is temperature independent and it corresponds to the expected formula for tunneling through a parabolic barrier. However, at high temperatures $T \gg T_0$ (small electrostatic energy), the behavior becomes that of thermal activation.

In case of a hexagonal close packaging of spherical nanoparticles, a layer of thickness $l$ contains $n = 3 l/(6^{1/2} \cdot d)$ monolayers, with $d$ being the diameter of the nanoparticles, $l \gg d$, that is, the applied voltage drops across a large number of junctions. On the contrary, the electric field enhancement at the junctions is expected to be in the order a factor $M$ equal to the ratio of the average size of the conducting grains $d$ to the average junction width $w$, $M \approx d/w$. Assuming for granular, nanosized SFMO–SMO core–shell structures $d = 75$ nm and $w = 1.24$ nm,[16] the resulting number $nd/w$ will be still very large. In the resulting low-voltage regime and supposing direct tunneling through thin enough barriers, the sheet resistance up to a factor $F$ is given by[24,26]

$$R_{0,sq.} = \frac{\pi^2 \hbar^2}{e^2 \sqrt{2m^* V_0} \cdot w} \tag{9}$$

Here, $F$ depends on the ratio of the reciprocal localization length $\chi$ and the wave vector of the wave function of the tunneling spin-down electrons $k_\downarrow$ as well as on the angle $\varphi$ between the magnetic moments of the two neighboring grains[26]

$$F = \frac{\chi^2(1 + k_\downarrow^2/\chi^2)^2}{k_\downarrow^2(1 + \cos\varphi)} \tag{10}$$

In granular films, tunneling of electrons occurs between neighboring grains whose magnetic moments are usually not parallel. For noninteracting grains, averaging over $\cos\theta$, where $\theta$ is the angle between the magnetization directions of two neighboring grains, results in[27]

$$\langle\cos\theta\rangle = m(B, T)^2 \tag{11}$$

Up to 150 K, $m(B,T)$ decreases in comparison with its low-temperature value by 10–12%.[1,21] Therefore, we assume a temperature-independent value of $m$ in the low-temperature region. Moreover, for the sake of simplicity, we will not take into account the magnetic flux dependence of the factor $F$ because $m(B,T)$ defines the value of $F$ within a factor of two.

In nanosized, granular SFMO–SMO core–shell structures, the barrier thickness is in the order of $w \approx 1/\chi$.[16] On the contrary, the barrier is much thinner than the magnetic length $l_B = (\hbar/eB)^{1/2}$. In this case, the barrier height was experimentally found to follow the relation[28]

$$V_0(B) = V_0(0) - \beta B + \gamma B^2 \tag{12}$$

The derived equations allow modeling of the temperature and field dependence of the tunneling magnetoresistivity.

## 3. Results and Discussion

SFMO resistivity was calculated in dependence on temperature $T$ and magnetic flux density $B$ by means of Equation (8) taking $T_1$ from Equation (3) and (4) and $T_0$ from Equation (6) and (7). Parameters used for calculations and corresponding references are shown in **Table 1**. The preexponential factor $\rho_0/F = 3.51 \times 10^4$ was evaluated combining Equation (9) and (10) for $\cos\theta \ll 1$ and $l = 1$ cm.

For ferromagnetic Fe, the Fermi surface of the itinerant $d_i$ electrons can be approximated by a sphere of radius $k_F = (3\pi n_e)^{1/3}$, where $n_e$ is the total electron density.[29] Such a very simple approximation yields $F \approx 26$ for SFMO. On the contrary, the Fermi surfaces of lanthanum manganite A-site substituted by one-third[30] as well as SFMO[31] are more complicated. SFMO is half-metallic where only down-spin states are active at

**Table 1.** Parameters used for model calculations.

| Parameter, dimension | Value | Ref. |
|---|---|---|
| $w$ [nm] | 1.24 | [16] |
| $A$ [nm$^2$] | 360 | [16] |
| $V_0$ [meV] | 13.2 | [16] |
| $m^*/m_e$ | 2.5 | [35] |
| $f$ | $\pi/2$ | – |
| $n_e$ [cm$^{-3}$] | $\sim 1 \times 10^{22}$ | [2,36,37] |
| $\beta$ [meV T$^{-1}$] | 1.16 | [28] |
| $\gamma$ [meV T$^{-2}$] | 0.040 | [28,33] |

the Fermi surface.[1] Around the Fermi level, these states consist of energetically overlapping Mo 4$d$ $t_{2g}$ and Fe 3$d$ $t_{2g}$ states hybridized with oxygen 2$p$ states. This complicates the calculation of $k_\downarrow$. Phenomenologically, we obtain a value of $F \approx 14$ by fitting of the resistivity in the absence of a magnetic field to data.[16] This value is reasonable because we have neglected disorder and charge scattering effects.

MR calculations were performed based on Equation (12). The coefficient $\beta$ was attributed in the study by López-Mir et al.[28] to Zeeman splitting amounting about 1 $\mu_B$ (1$\mu_B \approx 0.058$ meV T$^{-1}$) for a magnetic field perpendicular and about 18 $\mu_B$ for a magnetic field applied parallel to the current. In our case, the Fermi level of the down-spin states of SFMO is shifted up, while the levels of the SMO barrier remain constant. Thereby, the tunneling barrier is reduced. As a first estimate, the coefficient $\beta$ was chosen as $\beta = 20$ $\mu_B$. The coefficient $\gamma$ was determined from data in the study by López-Mir et al.[28] yielding $\gamma = 0.034$ meV T$^{-2}$. Note that the thickness of the La$_2$Co$_{0.8}$Mn$_{1.2}$O$_6$ layer in the study by López-Mir et al.[28] is in the order of the electron mean free path of a similar double perovskite.[32] This yields an anisotropy of MR and the tunneling current measured along film thickness direction with the field applied perpendicular and parallel to the sample. This anisotropy smears out in bulk samples where the electrons are scattered in all directions. A theoretical estimate of $\gamma$ following[33]

$$\gamma = \frac{z^2 e^2 B^2}{6m^*} \tag{13}$$

and supposing $z_{eff} = (\pi/4)^{1/2}d$, with $d = 75$ nm[16] results in $\gamma = 0.052$ meV T$^{-2}$. As we are not dealing with collision-free electrons, this value is obviously overestimated. Thus, we have fixed the value of $\gamma$ to 0.040 meV T$^{-2}$.

The temperature dependence of the resistivity calculated in dependence on $B$ is shown in **Figure 1**. Note that the zero field resistivity was fitted experimental data[16] by choosing an appropriate value of the factor $F$ to avoid problems in the calculation of $k_\downarrow$.
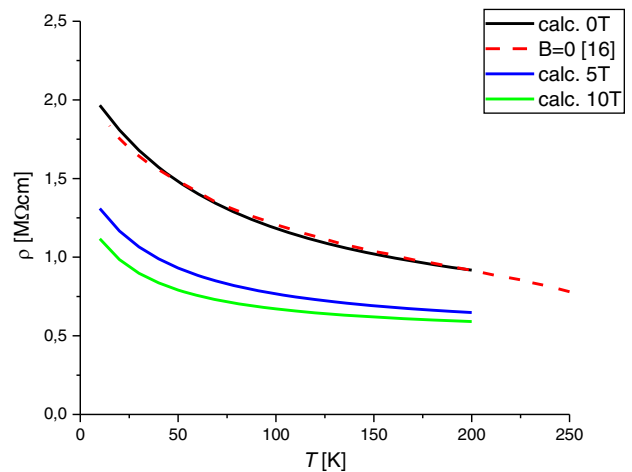


**Figure 1.** Temperature dependence of the resistivity of nanosized, granular SFMO–SMO core–shell structures in dependence on the magnetic flux density. For comparison, zero field data taken from Suchaneck et al.[16] are depicted as a dashed line.
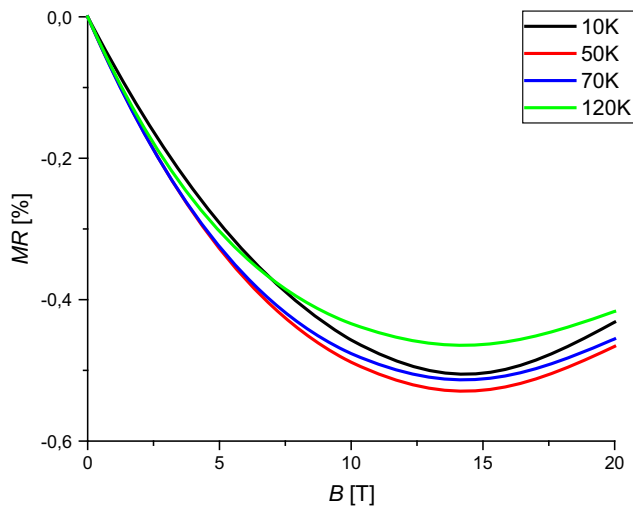
**Figure 2.** Calculated field dependence of the MR of nanosized, granular SFMO–SMO core–shell structures with temperature as parameter.



**Figure 3.** Calculated temperature dependence of the MR of nanosized, granular SFMO–SMO core–shell structures with magnetic flux density as parameter in comparison with experimental data of sintered, granular SFMO.[12]

**Figure 2** shows the magnetic flux density dependence of the MR

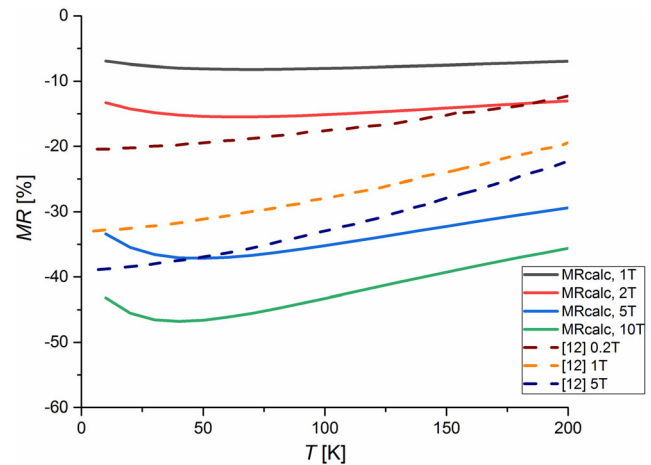$$\mathrm{MR} = \frac{\rho(B) - \rho(0)}{\rho(0)} \qquad (14)$$

calculated using Equation (8) with regard to Equation (12). The obtained negative MR is similar to the one of high-temperature sintered SFMO ceramics.[1,4–8] The predicted MR increases with increasing magnetic flux density. The decrease in MR with $B$ in very high magnetic fields is an artifact of the model attributed to the termination of the series expansion of Equation (12). The location of the minimum depends on the value $\gamma$. With decreasing $\gamma$, it shifts to higher fields. On the contrary, the predicted temperature dependence of the MR in nanosized, granular SFMO–SMO core–shell structure is much weaker than in the SFMO ceramics. This would be an advantage for device application near room temperature. The increase in the MR up to a temperature of 50 K followed by a decrease is in accordance with experimental data for granular SFMO samples which were attributed to the FIT model.[12]

**Figure 3** confirms that contrary to manganite[34] and SFMO ceramics,[1] the MR of nanosized, granular SFMO–SMO core–shell structures is only weakly temperature dependent. This is in qualitative agreement with experimental data of sintered, granular SFMO obeying the FIT model.[12]

The weak temperature dependence of the MR is a consequence of a temperature $T_0$ in the order of the temperature at resistivity measurements. In our example, $T_1 = 217$ K and $T_1/T_0 = 1.48$ under zero-field conditions decreasing to $T_1 = 46$ K and $T_1/T_0 = 0.97$ at $B = 10$ T, correspondingly. Note that our values of $T_0$ and $T_1/T_0$ are lower than the reported ones in the literature,[13,14] meaning that the MR field dependence of cold-pressed SFMO as well as sintered and grinded $Sr_2CrMoO_6$ ceramics could be even less.

## 4. Conclusion

A model for the MR in nanosized, granular SFMO–SMO core–shell structures was proposed for the first time. It is based on the FIT model of Sheng et al. MR was modeled by considering a magnetic field-dependent barrier height. The model predicts a MR up to about 50% and a weak temperature dependence of the MR. The latter is beneficial for spintronic device application near room temperature.

## Conflict of Interest

The authors declare no conflict of interest.

## Data Availability Statement

Data sharing is not applicable to this article as no new data were created or analyzed in this study.

[1] K. I. Kobayashi, T. Kimura, H. Sawada, K. Terakura, Y. Tokura, *Nature* **1998**, *395*, 677.

[2] Y. Tomioka, T. Okuda, Y. Okimoto, R. Kumai, K. Kobayashi, Y. Tokura, *Phys. Rev. B* **2000**, *61*, 422.

[3] L. I. Balcells, J. Navarro, M. Bibes, A. Roig, B. Martínez, J. Fontcuberta, *Appl. Phys. Lett.* **2001**, *78*, 781.

[4] D. Niebieskikwiat, F. Prado, A. Caneiro, R. D. Sánchez, *Phys. Rev. B* **2004**, *70*, 132412.

[5] J. F. Wang, Z. Li, X. J. Xu, Z. Bin Gu, G. L. Yuan, S. T. Zhang, *J. Am. Ceram. Soc.* **2014**, *97(4)*, 1137.

[6] A. Nag, S. Jana, S. Middey, S. Ray, *IOP Conf. Ser. Mater. Sci. Eng.* **2013**, *46*, 012001.

[7] D. Niebieskikwiat, A. Caneiro, R. D. Sánchez, J. Fontcuberta, *Phys. Rev. B* **2001**, *64*, 180406(R).

[8] N. Kalanda, D. H. Kim, S. Demyanov, S. C. Yu, M. Yarmolich, A. Petrov, S. K. Oh, *Curr. Appl. Phys.* **2018**, *18*, 27.

[9] H. Fujimori, S. Mitani, S. Ohnuma, *Mater. Sci. Eng. B* **1995**, *31*, 219.

[10] B. Fisher, K. B. Chashka, L. Patlagan, G. M. Reisner, *Phys. Rev. B* **2003**, *68*, 134420.

[11] B. Fisher, K. B. Chashka, L. Patlagan, G. M. Reisner, *Current Appl. Phys.* **2004**, *4*, 518.

[12] B. Fisher, K. B. Chashka, L. Patlagan, G. M. Reisner, *J. Magn. Magn. Mater.* **2004**, *272–276*, 1790.

[13] B. Fisher, J. Genossar, K. B. Chashka, L. Patlagan, G. M. Reisner, *Solid State Commun.* **2006**, *137*, 641.

[14] B. Fisher, J. Genossar, K. B. Chashka, L. Patlagan, G. M. Reisner, *EPJ Web Conf.* **2014**, *75*, 01001.

[15] S. Granville, I. L. Farrell, A. R. Hyndman, D. M. McCann, R. J. Reeves, G. V. M. Williams, arXiv:1707.01208 [cond-mat.mes-hall], **2017**.

[16] G. Suchaneck, N. Kalanda, E. Artsiukh, M. Yarmolich, N. A. Sobolev, *J. Alloys Compd.* **2020**, *860*, 158526.

[17] P. Raychaudhuri, T. K. Nath, A. K. Nigam, R. Pinto, *J. Appl. Phys.* **1998**, *84*, 2048.

[18] M. Saloaro, S. Majumdar, H. Huhtinen, P. Paturi, *J. Phys.: Condens. Matter* **2012**, *24*, 366003.

[19] A. Krichene, W. Boujelben, N. A. Shah, P. S. Solanki, *J. Alloys Compd.* **2020**, *820*, 153400.

[20] D. Serrate, J. M. De Teresa, P. A. Algarabel, M. R. Ibarra, J. Galibert, *Phys. Rev. B* **2005**, *71*, 104409.

[21] E. K. Hemery, G. V. M. Williams, H. J. Trodahl, *Physica B: Condens. Matter* **2007**, *390*, 175.

[22] N. G. Van Kampen, *Physica* **1960**, *26*, 585.

[23] P. Sheng, E. K. Sichel, J. I. Gittleman, *Phys. Rev. Lett.* **1978**, *40*, 1197.

[24] J. G. Simmons, *J. Appl. Phys.* **1963**, *34*, 1793.

[25] J. S. Helman, B. Abeles, *Phys. Rev. Lett.* **1976**, *37*, 1429.

[26] J. C. Slonczewski, *Phys. Rev. B* **1989**, *39*, 6995.

[27] J. Inoue, S. Maekawa, *Phys. Rev. B* **1996**, *53*, R11927(R).

[28] L. López-Mir, C. Frontera, H. Aramberri, K. Bouzehouane, J. Cisneros-Fernández, B. Bozzo, L. Balcells, B. Martínez, *Sci. Rep.* **2018**, *8*, 861.

[29] M. B. Stearns, *J. Magn. Magn. Mater.* **1977**, *5*, 167.

[30] W. E. Pickett, D. J. Singh, *J. Magn. Magn. Mater.* **1997**, *172*, 237.

[31] M. G. Yamada, G. Jackeli, *Phys. Rev. Mater.* **2020**, *4*, 074007.

[32] D. Mazur, K. E. Gray, J. F. Zasadzinski, L. Ozyuzer, I. S. Beloborodov, H. Zheng, J. F. Mitchell, *Phys. Rev. B* **2007**, *76*, 193102.

[33] B. I. Shklovskii, A. L. Efros, *Sov. Phys. JETP* **1983**, *57*, 470.

[34] H. Y. Hwang, S. Cheong, N. P. Ong, B. Batlogg, *Phys. Rev. Lett.* **1996**, *77*, 2041

[35] T. Saitoh, M. Nakatake, H. Nakajima, O. Morimoto, A. Kakizaki, S. Xu, Y. Moritomo, N. Hamada, Y. Aiura, *Phys. Rev. B* **2005**, *72*, 045107.

[36] W. Westerburg, D. Reisinger, G. Jakob, *Phys. Rev. B* **2000**, *62*, R767.

[37] H. Yanagihara, M. B. Salamon, Y. Lyanda-Geller, S. Xu, Y. Moritomo, *Phys. Rev. B* **2001**, *64*, 214407.